

Domain growth in binary mixtures at low temperatures

A. M. Lacasta, A. Hernández-Machado, and J. M. Sancho

Departamento de Estructura y Constituyentes de la Materia, Universidad de Barcelona, Avenida Diagonal, 647, E-08028 Barcelona, Spain

R. Toral

Department de Física, Universitat de les Illes Balears, E-07071 Palma de Mallorca, Spain

(Received 17 May 1991; revised manuscript received 23 August 1991)

We have studied domain growth during spinodal decomposition at low temperatures. We have performed a numerical integration of the deterministic time-dependent Ginzburg-Landau equation with a variable, concentration-dependent diffusion coefficient. The form of the pair-correlation function and the structure function are independent of temperature but the dynamics is slower at low temperature. A crossover between interfacial diffusion and bulk diffusion mechanisms is observed in the behavior of the characteristic domain size. This effect is explained theoretically in terms of an equation of motion for the interface.

I. INTRODUCTION

Domain growth during phase separation is an interesting pattern formation phenomenon.¹ This situation appears, for example, in spinodal decomposition. In this case, a system that is initially in a homogeneous phase is suddenly quenched inside the coexistence region. Then, the homogeneous phase becomes unstable and it evolves spontaneously by generating domains of the new equilibrium phases. At a late stage, the evolution of the pattern can be described by the relaxational motion of the convoluted interface separating the domains. Examples of these dynamic processes have been studied experimentally in binary mixtures, like binary liquids and alloys.¹

From the theoretical point of view, apart from microscopic models, these processes have been described by time-dependent Ginzburg-Landau equations for the concentration, a conserved order parameter. Recently, some attention has been focused on the modification of these equations by considering a concentration-dependent diffusion coefficient instead of the usual assumption of constant diffusion.²⁻¹¹ First, Langer² and Kitahara and Imada³ have pointed out that this modification is necessary for a correct modeling of a deep quench. More recently, Kitahara *et al.*⁴ and Jasnow⁵ have also commented on the necessity of this assumption if the effect of external fields, like gravity, is to be taken into account. They have studied the effects of a gravitational field on the dynamics of spinodal decomposition by using a cell model.⁴ Puri and Oono⁶ have briefly commented on the implications of this assumption on the growth laws in spinodal decomposition. Ohta⁷ and Shiwa⁸ have derived interfacial equations without and with external field, respectively. Furthermore, from the point of view of fluctuations, the generalization of the assumption on the diffusion coefficient opens interesting possibilities and raises questions regarding the role of noise and the way in which it has to be introduced into the equations. In gen-

eral, the derivations of modified stochastic Ginzburg-Landau equations from more mesoscopic models, like master equations, give as a result the presence of multiplicative noise. In the small-noise limit, a mesoscopic derivation of macroscopic equations and equations for fluctuations with additive noise has been obtained.⁹ Before we study the effect of fluctuations in these systems, it is essential to understand the deterministic domain growth and the mechanisms involved in it.

In this paper we concentrate on the effects of a concentration-dependent diffusion coefficient on the deterministic dynamics of spinodal decomposition, as a modeling of deep quench. We present results from a numerical integration of the modified Ginzburg-Landau equation. Starting from random initial conditions, we have observed a delay of the domain-growth dynamics with respect to the constant diffusion case. We have studied numerically the behavior of the spatial correlation function, structure function, and characteristic domain size. The algebraic behavior of the characteristic size seems to change continuously with time from a $\frac{1}{4}$ - to a $\frac{1}{3}$ -power law. The crossover from one value to the other appears at longer times for lower temperatures and occurs at infinite time for zero temperature. We are interested in the characterization of this crossover regime. We find that, after a transient, the pair-correlation function and the structure function versus rescaled lengths seem to present a form which is independent of temperature and time. In this sense, patterns at different times with the same domain size are statistically equivalent. The crossover behavior can be understood in terms of the equation describing the motion of the interface.^{7,12} From this equation, we propose an evolution equation for the characteristic domain size. This equation contains two terms related with a surface diffusion and a bulk diffusion mechanism, respectively. The first one dominates at short times whereas the second dominates at long times. We have obtained an expression for the critical domain

size which determines this crossover. The derivation of the equations which contain multiplicative noise and the study of the role of noise in this case is in progress.

In Secs. II and III we present our numerical and analytical results, respectively. In the Appendix, we derive briefly the interfacial equation. Our conclusions are summarized in Sec. IV.

II. MODEL AND NUMERICAL RESULTS

Our macroscopic continuous model is given by the following dynamic equation for the concentration $\bar{c}(\mathbf{r}, \tau)$:

$$\frac{\partial}{\partial \tau} \bar{c}(\mathbf{r}, \tau) = \nabla \Gamma(\bar{c}) \cdot \nabla \frac{\delta F(\{\bar{c}\})}{\delta \bar{c}}, \quad (2.1)$$

where $F(\{\bar{c}\})$ is the Ginzburg-Landau free energy

$$F(\{\bar{c}\}) = \int d\mathbf{r} \left[-\frac{r\bar{c}^2}{2} + \frac{u\bar{c}^4}{4} + \frac{\kappa(\nabla\bar{c})^2}{2} \right]. \quad (2.2)$$

To account for deep quench and also for phase separation dynamics in the presence of a gravitational field, a variable-dependent diffusion coefficient, $\Gamma(\bar{c})$, has been proposed.²⁻⁴ Based on phenomenological arguments, the form of $\Gamma(\bar{c})$ is²⁻⁴

$$\Gamma(\bar{c}) = \Gamma_0(\bar{c}_0^2 - \bar{c}^2), \quad (2.3)$$

where Γ_0 is a constant, $\bar{c}_0 = \bar{c}_{st}(T=0)$ and $\bar{c}_{st}(T)$ is the equilibrium value for temperature T . Equation (2.3) takes into account the decrease in the bulk diffusion by reducing temperature. In particular, $\Gamma(\bar{c})=0$ at $T=0$, except at the interface. Then, at low temperatures, diffusion along the interfaces between domains (surface diffusion) becomes important.

Equation (2.1) can be written in the dimensionless form¹³

$$\frac{\partial c}{\partial t} = \frac{1}{2} \nabla(1 - \alpha c^2) \cdot \nabla \left[-\nabla^2 c + \frac{df}{dc} \right], \quad (2.4)$$

$$f(c) = -\frac{c^2}{2} + \frac{c^4}{4}, \quad (2.5)$$

where $\alpha = [\bar{c}_{st}(T)/\bar{c}_0]^2$ is the only relevant parameter in our study. Its values go from 0 to 1 as temperature is reduced, and $\alpha=1$ for $T=0$. Now the bulk equilibrium values of the variable are $c_{st} = \pm 1$.

In our numerical simulation, we have considered the discretization of Eq. (2.4) in a square lattice of $N \times N$ points, with $N=120$ and periodic boundary conditions. We have integrated numerically this equation using Euler's method with a spatial mesh size $(\Delta x, \Delta y) = (1, 1)$ and a time step $\Delta t = 0.025$.¹³⁻¹⁵ The time step and mesh size are sufficiently large that one could say that we are not solving the partial differential equation but simulating some kind of coarse-grained model like cell models.⁶ However, we have checked that for smaller values of these parameters our conclusions remain the same. The gradient operators in Eq. (2.4) have been discretized according to a prescription which makes the right-hand side of (2.4) symmetric:

$$\nabla f(c) \cdot \nabla g(c) = \frac{1}{2} [\nabla_R f(c) \cdot \nabla_L g(c) + \nabla_L f(c) \cdot \nabla_R g(c)], \quad (2.6)$$

where ∇_R and ∇_L are the discrete versions of the right and left gradients, respectively. Our initial distribution for the concentration, $c(\mathbf{r}, 0)$, is chosen uniformly random in the interval $(-\epsilon_0, \epsilon_0)$ with $\epsilon_0=0.05$. The results have been averaged over 10 runs up to a maximum $t=21000$.

In order to study the dynamic behavior of the domain growth, we introduce the pair-correlation function

$$G(\mathbf{r}, t) = \frac{1}{N^2} \sum_{\mathbf{r}'} \langle c(\mathbf{r} + \mathbf{r}', t) c(\mathbf{r}', t) \rangle. \quad (2.7)$$

The brackets mean an average over initial conditions. Since our system is isotropic, G depends only on the modulus of \mathbf{r} . Then, a circular average on $G(\mathbf{r}, t)$ will lead to the radial pair-correlation function

$$g(r, t) = \frac{1}{N_r} \sum_{\theta} G(\mathbf{r}, t), \quad (2.8)$$

where the sum runs over the set θ of points inside a corona of radius r and $r + \Delta r$. N_r is the number of such points. As usual, we also define a relevant length $R_g(t)$ as the smallest value of r for which g becomes zero.

We also introduce the structure function

$$S(\mathbf{k}, t) = \sum_{\mathbf{r}} e^{i\mathbf{k} \cdot \mathbf{r}} G(\mathbf{r}, t). \quad (2.9)$$

Because of the radial symmetry of the system, we will introduce the spherically averaged structure function

$$s(k, t) = \frac{1}{N_k} \sum_{\theta} S(\mathbf{k}, t), \quad (2.10)$$

where the sum runs over the set of points inside a corona of radius k and $k + \Delta k$ and N_k is the number of such points.

Here, our main interest is to determine how the phase separation dynamics given by Eq. (2.4) depends on the parameter α . We have integrated Eq. (2.4) for five different values of α . In Fig. 1, we present the results for $g(r, t)$:

$$g(r, t) = g(r/R_g(t)). \quad (2.11)$$

Furthermore, we also present the results for scaled structure function in Fig. 2:

$$s(kR_g(t)) = [R_g(t)]^{-2} s(k, t). \quad (2.12)$$

First, we have tested that our numerical scheme reproduces the well-known results of the scaling regime for $\alpha=0$.¹⁵ In Fig. 1, we present results for the smallest values of time for which the pair-correlation function presents a behavior independent of temperature. We find that the form of the pair-correlation function, Eq. (2.11), is independent of α within our numerical accuracy. This form coincides with the asymptotic results of Ref. 15 which are the longest simulations available using Euler's method. This implies that the parameter α , even for $\alpha=1$, does not affect this important aspect of the phase

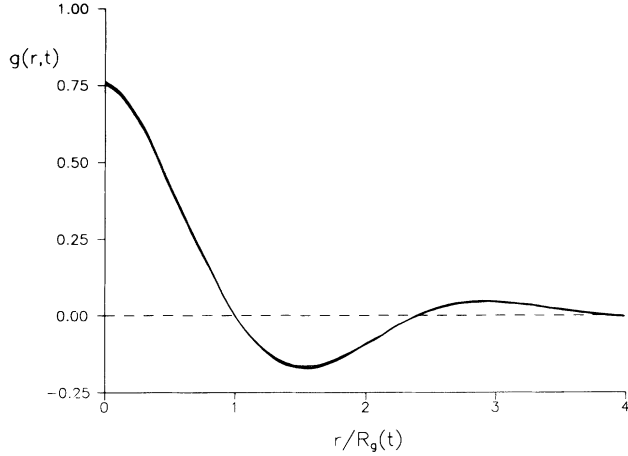


FIG. 1. Radial correlation function, Eq. (2.8), vs the scaled variable $r/R_g(t)$, for five values of α . The curves have been taken at times $t = 1200$ for $\alpha = 0$, $t = 1400$ for $\alpha = 0.2$, $t = 2000$ for $\alpha = 0.6$, $t = 3000$ for $\alpha = 0.8$, and $t = 5800$ for $\alpha = 1$.

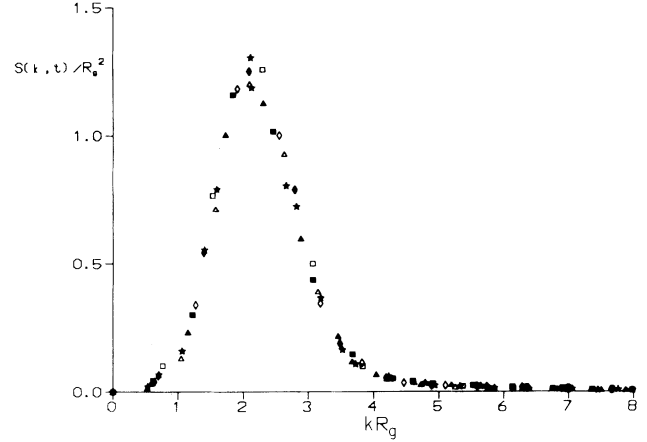


FIG. 2. Scaled radial structure function, Eq. (2.12), vs the scaled variable $kR_g(t)$, for two values of α ($\alpha = 0$, solid symbols; $\alpha = 0.8$, open symbols). The points have been taken at times 5000 (\star), 8000 (\blacksquare), 10 000 (\blacktriangle), 12 000 (\blacklozenge); 9000 (\star), 12 000 (\square), 15 000 (\triangle), 18 000 (\diamond).

separation dynamics. However, $R_g(t)$ does depend on it. Furthermore, we observe that patterns for different α but corresponding to the same R_g have a similar morphology. This implies that the characteristic morphology of the phase separation dynamics remains unchanged by temperature. In Fig. 2, we present results for the structure function for two different values of α . We obtain that, for the times considered, larger than in Fig. 1, this function is independent of temperature and time.

Now, we concentrate on the behavior of R_g . In Fig. 3 we present a plot of $\ln R_g(t)$ vs $\ln t$, for values up to $t = 21\,000$. We have analyzed these data by a nonlinear fit of the form $R_g(t) = \beta_2 + \beta_1 t^n$. In Table I, we present our results for the exponent n for the best fit obtained by minimizing the χ^2 function.¹⁵ In Fig. 3, we have considered a temporal regime for which our results for $\alpha = 0$ are already in agreement with the Lifshitz-Slyozov theory ($n = \frac{1}{3}$).¹³⁻¹⁷ However, the results for other values of α

still seem to depend on α . For these cases, inspection of Fig. 3 shows that the slope is continuously changing with time and approaching the $\frac{1}{3}$ value for long times. The approach is slower when α approaches 1. For $\alpha = 1$ the slope is always around $\frac{1}{4}$. Similar results are obtained from the so-called effective exponent defined by

$$n_{\text{eff}}(\alpha) = \frac{\ln[R_g(\alpha t)/R_g(t)]}{\ln \alpha}, \quad (2.13)$$

where α is an arbitrary number. In Fig. 4 we see how n_{eff} behaves as a function of $1/R_g$ for different values of α . For $\alpha = 0$ our simulation is in agreement with the prediction that n_{eff} should approach $\frac{1}{3}$ from below for $R_g \rightarrow \infty$.¹⁶ But for $\alpha \neq 0$ the results also change with α in the same way as in Fig. 3. The interpretation of these results in terms of a crossover between different growth mechanisms is considered in the next section.

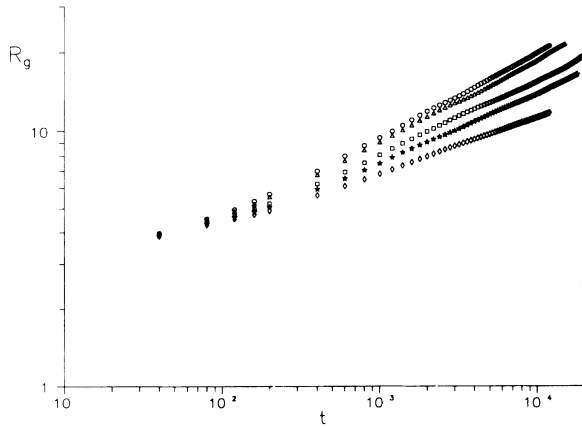


FIG. 3. log-log plot of the time evolution of $R_g(t)$ for the same five values of Fig. 1. [$\alpha = 0$, (\circ), $\alpha = 0.2$ (\triangle), $\alpha = 0.6$ (\square), $\alpha = 0.8$ (\star), $\alpha = 1$ (\diamond).

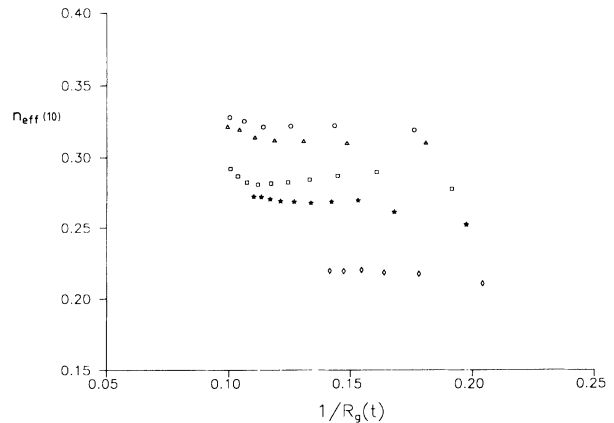


FIG. 4. Effective exponents defined in (2.9) vs $1/R_g(t)$. The symbols correspond to the same values in Fig. 3.

TABLE I. Table of our numerical results for the parameters involved in the power-law behavior of the domain size $R_g(t)$.

α	n	A	B	$C_2 = A/(1-\alpha)$	$C_3 = B/\alpha$	l_c	$x_1(l < l_c)$	$x_2(l > l_c)$
0	0.33±0.01	0.27±0.02	-0.1±0.2	0.27±0.02		0		0.33±0.01
0.2	0.33±0.01	0.25±0.02	-0.4±0.2	0.31±0.02		~0		0.33±0.01
0.6	0.30±0.02	0.10±0.01	0.34±0.03	0.25±0.03	0.57±0.05	3.4±0.5		0.30±0.02
0.8	0.28±0.01	0.04±0.01	0.50±0.05	0.20±0.03	0.62±0.06	12±2	0.26±0.01	0.30±0.01
1	0.22±0.01	0.00±0.01	0.5±0.1		0.5±0.1	∞	0.22±0.01	

III. INTERFACIAL DYNAMICS

A theoretical explanation of our numerical results can be obtained from the interfacial equation which describes the evolution of the domains. This equation was obtained by Ohta⁷ using a projection technique.¹² In the Appendix, we briefly present a rederivation following a scheme given in Ref. 13 for $\Gamma(c) = \Gamma_0$. Equation (2.4) can be written in a more useful form:⁷

$$\frac{\partial c}{\partial t} = (1-\alpha)\nabla^2 \left[-\nabla^2 c + \frac{df}{dc} \right] + \alpha\nabla(1-c^2) \cdot \nabla \left[-\nabla^2 c + \frac{df}{dc} \right]. \quad (3.1)$$

The first term on the right-hand side (rhs) of Eq. (3.1) is responsible for the usual bulk diffusion mechanism but now with an effective diffusion coefficient $(1-\alpha)$. The second term on the right-hand side of Eq. (3.1) is responsible for the interfacial diffusion mechanism. As explained in the Appendix, it gives rise to a contribution to the total flux which does not appear for $\alpha=0$. It is only important at the interface and only the tangential component gives a relevant contribution. When $\alpha=0$ only the bulk diffusion term survives but when $\alpha=1$ this mechanism is inhibited and the interfacial diffusion mechanism will be dominant. For intermediate values for α one can expect a crossover behavior which will allow us to interpret the numerical results observed in the simulation.

From Eq. (A9) of the Appendix, it is possible to write an equation for the normal component of the velocity:⁷

$$4v(s,t) = (1-\alpha)\sigma \int ds' W(r(s), r(s')) K(s,t) + 4\alpha\nabla^2 K(s,t), \quad (3.2)$$

where K is the local curvature, Eq. (A3), v is the normal velocity, Eq. (A6), σ is the surface tension, Eq. (A10), and G is the Green function solution of Eq. (A8). W is defined by the following equation:

$$\int ds'' G(r(s), r(s'')) W(r(s''), r(s')) = \delta(s-s'). \quad (3.3)$$

The first and second terms on the rhs of Eq. (3.2) contain the bulk and interfacial mechanisms of growth, respectively. This is an important difference regarding the usual constant diffusion model for which this derivation gives only bulk diffusion ($\alpha=0$).¹³ For this last model it has been claimed that interfacial diffusion (surface diffusion) is also present and responsible for the transient

behavior observed in numerical integrations. However, this argument has not been substantiated, to our knowledge, by a derivation from any field model.^{14,15} In fact, in our derivation, an assumption of a variable-dependent diffusion coefficient is required to yield such an interfacial diffusion mechanism. Now, it is simple to obtain from dimensional arguments the power-law behavior for the domain size associated to the different mechanisms. We obtain a $\frac{1}{4}$ -power law for $\alpha=1$ and $\frac{1}{3}$ -power law for $\alpha=0$. For intermediate values of α there is a crossover behavior between these two values in accordance with the numerical results in Figs. 3 and 4. For intermediate values of α , the exponent $\frac{1}{3}$ should dominate for long enough times. We would like to determine qualitatively the value of the critical domain size for which the crossover occurs. From Eq. (3.2) it seems natural to propose the following equation for the characteristic domain size $R(t)$:

$$\frac{dR(t)}{dt} = (1-\alpha)\frac{C_2}{R^2} + \alpha\frac{C_3}{R^3}, \quad (3.4)$$

where the first and second terms on the rhs of Eq. (3.4) take into account the bulk and interfacial diffusion mechanisms, respectively. We can estimate qualitatively the crossover by comparing the two terms of Eq. (3.4). We can define a critical domain size l_c as that for which the two contributions of Eq. (3.4) are equal. Then we can write

$$l_c = \frac{C_3}{(1/\alpha-1)C_2}. \quad (3.5)$$

Constants C_2 and C_3 can be obtained from our numerical results for $R_g(t)$. Due to the very large errors involved in the numerical calculation of the derivative of an oscillating $R_g(t)$,^{15,17} we have considered two different numerical methods that give consistent results in the margin of the error bars. The first one takes into account that Eq. (3.4) predicts a straight-line behavior for $R^2 dR/dt = A + B/R$ vs $1/R$. Then, by means of a linear fit, we have estimated the parameter $A = (1-\alpha)C_2$ and the rate $B = \alpha C_3$. As a second method, we have solved the ordinary differential equation (3.4) in terms of an initial condition and we have fitted the data of Fig. 3. We present the results for A and B and also for C_2 and C_3 in Table I. In particular, we see that C_2 and C_3 are more or less constant within our error bars. Ohta⁷ has given an expression for l_c . His result reduces to Eq. (3.5) for $C_2 = C_3$. As we see from Table I, it gives lower values of l_c than those of our simulation.

Now, we can interpret our numerical results in terms of the crossover implied by Eq. (3.4) and of a critical domain size. In this way we can obtain a better estimation of the dynamical exponent from our numerical results by fitting our data for $R_g(t)$ vs $A_1 + B_1 t^x$ for two different intervals $l < l_c$ and $l > l_c$ separately. As can be seen from Table I, when $\alpha = 0.8$, the exponent is close to $\frac{1}{4}$ for $l < l_c$ but close to $\frac{1}{3}$ for $l > l_c$ in accordance with our theoretical analysis. For values of $\alpha < 0.7$, our results are always in the region $l > l_c$. For $\alpha = 1$ the critical domain size is always in the region of $l < l_c$.

IV. CONCLUSIONS

We have studied, both numerically and analytically, the effects of a concentration-dependent diffusion coefficient on the domain-growth dynamics of a deterministic time-dependent Ginzburg-Landau model. We observe that the morphology of the patterns remains unchanged but there is a clear delay in the dynamics. We obtain that the characteristic domain size presents a crossover from $\frac{1}{4}$ - to $\frac{1}{3}$ -power law as a function of time. These results can be intuitively understood in terms of a reduction in the bulk diffusion mechanism that induces a greater role of interfacial diffusion for short times. These results are confirmed by previous analytical results from Ohta and by the analytical results that we have presented here. In our derivation we can associate the present interfacial mechanism with the presence of a tangential flux at the interface. This flux increases as temperature is reduced. The crossover between the two mechanisms appears later at lower temperatures, but the long-time behavior is finally dominated by bulk diffusion in accordance with Lifshitz-Slyozov theory. We give a qualitative estimation of the crossover through the introduction of a critical characteristic domain size. The theoretical model used here contains both interfacial and bulk diffusion mechanisms of growth. This is an important difference regarding the usual constant diffusion model for which only bulk diffusion is present. Our explanation of the origin of the effective exponents could be profitable in the interpretation of real experiments and other computer simulations, where it is very difficult to observe the exponents predicted by asymptotic theories.

ACKNOWLEDGMENTS

We are grateful to David Jasnow, T. Rogers, C. Yeung, and L. Ramírez-Piscina for illuminating discussions. A.H.M. and J.M.S. acknowledge NATO for financial support under a Collaborative Research Grant No. 900328. We also acknowledge financial support from Dirección General de Investigación Científica y Técnica (Spain) (Project Nos. PB90-0030 and PB89-0424).

APPENDIX: DERIVATION OF THE INTERFACIAL EQUATION

We introduce curvilinear coordinates (u, s) in Eq. (3.1), where s follows the contour of the interface and u goes along the normal direction of it, taking the value $u = 0$ at

the center of the interface. We separate $c(\mathbf{r}, t)$ into two parts

$$c(\mathbf{r}, t) = c_{st}(u(\mathbf{r}, t)) + \delta c(\mathbf{r}, t), \quad (\text{A1})$$

where c_{st} is the one-dimensional equilibrium profile of (3.1),

$$c_{st}(u) = \tanh \left[\frac{u}{\sqrt{2}} \right] \quad (\text{A2})$$

and δc is the deviation with respect to this solution. We assume that, after a transient regime, the interface profile, Eq. (A2), is well established and δc is a small quantity which does not depend on time (quasistatic approximation). Then, the pattern dynamics is given by the macroscopic motion of the interface, the local curvature of which becomes smaller as it evolves, as is defined as

$$K(\mathbf{r}, t) = -\nabla^2 u(\mathbf{r}, t). \quad (\text{A3})$$

Here we are considering the regime for which $K^{-1} \gg 1$. By substituting Eq. (A1) into (3.1), we obtain, to first order in δc ,

$$-v \frac{dc_{st}}{du} = (1 - \alpha) \nabla^2 \left[\mathcal{L} \delta c - K \frac{dc_{st}}{du} \right] + \alpha \nabla(1 - c_{st}^2) \nabla \left[\mathcal{L} \delta c - K \frac{dc_{st}}{du} \right], \quad (\text{A4})$$

where \mathcal{L} is a linear operator given by

$$\mathcal{L} = \frac{d^2 f}{dc_{st}^2} - \nabla^2 \quad (\text{A5})$$

and we have introduced the normal velocity v ,

$$v(\mathbf{r}, t) = -\frac{\partial u(\mathbf{r}, t)}{\partial t}. \quad (\text{A6})$$

In Eq. (A4) we have ruled out contributions of order K^2 . The derivative dc_{st}/du which appears in (A4) is the so-called Goldstone mode which is a sharply peaked function centered at the interface and with a width equal to 1. The Goldstone mode is an eigenfunction of (A5) with a zero eigenvalue and is associated with the interfacial degrees of freedom. We are looking for a description in which the degrees of freedom associated to the bulk (δc) are orthogonal to the interfacial ones. This requirement is accomplished if δc is given in terms of all the eigenfunctions, with the exception of the Goldstone mode, of the linear operator (A5) which, in the lowest order in K , is given by¹³

$$\mathcal{L} = \frac{d^2 f}{dc_{st}^2} - \frac{\partial^2}{\partial s^2} - \frac{\partial^2}{\partial u^2}. \quad (\text{A7})$$

After multiplying Eq. (A4) by the Green function solution of the equation

$$\nabla^2 G(\mathbf{r}, \mathbf{r}') = \delta(\mathbf{r} - \mathbf{r}') \quad (\text{A8})$$

and by the Goldstone mode and integrating over u , u' , and s' , the terms with a dependence on δc in Eq. (A4) do

not give any contribution. The resulting integrodifferential equation for the evolution of the interface described by its normal velocity and curvature K is

$$4 \int ds' G(\mathbf{r}(s), \mathbf{r}(s')) v(s', t) \\ = (1 - \alpha) \sigma K(s, t) + 4\alpha \int ds' G(\mathbf{r}(s), \mathbf{r}(s')) \nabla^2 K(s, t), \quad (\text{A9})$$

where σ is the surface tension

$$\sigma = \int_{-\infty}^{\infty} du \left[\frac{dc_{st}(u)}{du} \right]^2. \quad (\text{A10})$$

To get Eq. (A9) we have taken into account that the interfacial width is small in comparison with K^{-1} and one can approximate (A2) by a step function between the two equilibrium values ± 1 . As a consequence, the Goldstone mode can be substituted by a δ function.

At this point, we can make some comments regarding the different contributions on the rhs of Eq. (A4) to the final equation (A9). For $\alpha = 0$, Eq. (A9) is the usual interfacial equation.¹³ The most relevant contribution of $\alpha \neq 0$ comes from the second term on the rhs of Eq. (A4) and gives rise to the second term in Eq. (A9). The term in Eq. (A4) contains a flux localized at the interface. In our approximation, it can be expressed in terms of the components associated to the normal ($\hat{\mathbf{n}}$) and tangential direction ($\hat{\mathbf{t}}$) to the interface by

$$\nabla \left[K(s) \frac{dc_{st}}{du} \right] \sim K \frac{d^2 c_{st}}{du^2} \hat{\mathbf{n}} + \frac{dK}{ds} \frac{dc_{st}}{du} \hat{\mathbf{t}}. \quad (\text{A11})$$

The only contribution at our level of approximation is given by the tangential component of Eq. (A11).¹⁸ From Eq. (A9), we obtain that the equation for the normal component of the velocity is given by Eq. (3.2).

¹J. D. Gunton, M. San Miguel, and P. S. Shani, in *Phase Transitions and Critical Phenomena*, edited by C. Domb and J. L. Lebowitz (Academic, New York, 1983), Vol. 8, p. 267, and references therein.

²J. S. Langer, M. Bar-on, and H. D. Miller, *Phys. Rev. A* **11**, 1417 (1975).

³K. Kitahara and M. Imada, *Prog. Theor. Phys. Suppl.* **64**, 65 (1978).

⁴K. Kitahara, Y. Oono, and D. Jasnow, *Mod. Phys. Lett. B* **2**, 765 (1988).

⁵D. Jasnow, in *Far from Equilibrium*, edited by L. Garrido, *Lectures Notes in Physics* Vol. 319 (Springer-Verlag, Berlin, 1988).

⁶S. Puri and Y. Oono, *Phys. Rev. A* **38**, 1542 (1988).

⁷T. Ohta, *J. Phys. C* **21**, L361 (1988).

⁸Y. Shiwa, *Physica A* **148**, 414 (1988).

⁹A. Hernández-Machado and J. M. Sancho, *Phys. Rev. A* **42**, 6234 (1990).

¹⁰After this work was completed the work by C. Yeung (Ph.D.

thesis, University of Illinois, 1989) on the study of the effects of concentration-dependent diffusion coefficient in spinodal decomposition by a cell model algorithm (Ref. 11) came to our notice. The conclusions of this work on the universality of the morphology are similar to ours.

¹¹Y. Oono and P. Puri, *Phys. Rev. A* **38**, 434 (1988).

¹²K. Kawasaki and T. Ohta, *Prog. Theor. Phys.* **68**, 129 (1982).

¹³T. Rogers, Ph.D. thesis, University of Toronto, 1989.

¹⁴T. M. Rogers, K. R. Elder, and R. C. Desai, *Phys. Rev. B* **37**, 9638 (1988).

¹⁵E. T. Gawlinski, J. Viñals, and J. D. Gunton, *Phys. Rev. B* **39**, 7266 (1989).

¹⁶D. A. Huse, *Phys. Rev. B* **34**, 7845 (1986).

¹⁷R. Toral, A. Chakrabarti, and J. D. Gunton, *Phys. Rev. Lett.* **60**, 2311 (1988).

¹⁸In the derivation of this term by Ohta (Ref. 7), a supplementary spatial average in the direction to the interface is required. In our derivation, this average is not necessary.